ROYAL SOCIETY OF CHEMISTRY

PAPER

CrossMark
← click for updates

Unravelling the fundamentals of thermal and chemical expansion of BaCeO₃ from first principles phonon calculations

Andreas Løken, Reidar Haugsrud and Tor S. Bjørheim*

Differentiating chemical and thermal expansion is virtually impossible to achieve experimentally. While thermal expansion stems from a softening of the phonon spectra, chemical expansion depends on the chemical composition of the material. In the present contribution, we, for the first time, completely decouple thermal and chemical expansion through first principles phonon calculations on BaCeO₃, providing new fundamental insights to lattice expansion. We assess the influence of defects on thermal expansion, and how this in turn affects the interpretation of chemical expansion and defect thermodynamics. The calculations reveal that the linear thermal expansion coefficient is lowered by the introduction of oxygen vacancies being 10.6×10^{-6} K^{-1} at 300 K relative to 12.2×10^{-6} K^{-1} for both the protonated and defect-free bulk lattice. We further demonstrate that the chemical expansion coefficient upon hydration varies with temperature, ranging from 0.070 to 0.115 per mole oxygen vacancy. Ultimately, we find that, due to differences in the thermal expansion coefficients under dry and wet conditions, the chemical expansion coefficients determined experimentally are grossly underestimated – around 55% lower in the case of 10 mol% acceptor doped BaCeO₃. Lastly, we evaluate the effect of these volume changes on the vibrational thermodynamics.

1. Introduction

Mismatch between the functional components of a device as a consequence of thermal and chemical expansion can be detrimental for the overall performance and durability, and a detailed understanding of the origins of these expansion mechanisms is thus essential. The linear chemical expansion coefficient, ε_i, of a crystalline material along the *a*-, *b*- or *c*-axis can, for a given defect *i*, be described by

$$\varepsilon_i = \frac{1}{\delta_i}\left(\frac{l_i(T) - l_0(T)}{l_0(T)}\right) \quad (1)$$

where δ_i is the defect concentration given as the number of defects per formula unit, whereas $l_i(T)$ and $l_0(T)$ are the dimensions of the defective and perfect supercells, respectively. For proton conductors such as acceptor doped BaZrO₃ and BaCeO₃, these defects consist of protons (OH$_O^\bullet$) and oxygen vacancies (v$_O^{\bullet\bullet}$), where the hydration equilibrium

$$H_2O(g) + v_O^{\bullet\bullet} + O_O^\times \rightleftharpoons 2OH_O^\bullet \quad (2)$$
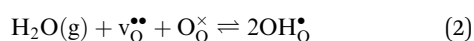
describes their relative dominance. In addition to a chemical expansion stemming from variations in the defect

Department of Chemistry, University of Oslo, FERMiO, Gaustadalléen 21, NO-0349 Oslo, Norway. E-mail: reidar.haugsrud@smn.uio.no

concentrations, materials are also subject to thermal expansion;

$$\alpha_i = \frac{1}{l}\frac{\partial l}{\partial T} \quad (3)$$

where α_i is the linear thermal expansion coefficient along one of the unit cell axes. While chemical expansion depends on the chemical composition of the material, thermal expansion originates from a softening of the phonon spectra of the lattice. Together, these two expansion processes, (1) and (3), comprise the thermochemical expansion.

The two expansion coefficients (ε_i and α_i) are usually determined simultaneously from structural measurements, *e.g.* X-ray powder diffraction or dilatometry, followed by subsequent measurements to determine the specific defect chemical concentrations, *e.g.* thermogravimetry or coulometric titration. This often entails assuming that α_i is constant throughout the temperature interval investigated, *i.e.* the thermal volume expansion is independent of any chemical reactions occurring (hydration in the case of proton conductors). Such an assumption can obviously lead to an under- or overestimation of the chemical expansion coefficient (ε_i) if α_i itself is changing. Recent experimental work on proton conducting BaCeY$_{0.2}$O$_{3-\delta}$[1] and BaCe$_{0.2}$Zr$_{0.7}$Y$_{0.1}$O$_{3-\delta}$[2] showed that the thermal expansion coefficient is higher when the material is hydrated under wet

relative to dry conditions, changing from 11.1×10^{-6} K to 9.9×10^{-6} K and 15.0×10^{-6} K to 12.7×10^{-6} K, respectively. However, in both cases, these differences were neglected, and chemical expansion coefficients were extracted assuming a constant thermal expansion coefficient. Such an assumption has also been employed for the chemical expansion due to oxidation of several oxide ion conductors in recent work by Marrocchelli *et al.*[3–7] In the present contribution, we will through quasiharmonic first principles phonon calculations, address the validity and consequences of this assumption by decoupling the thermal and chemical expansion mechanisms, ultimately providing new fundamental insights to lattice expansion. This will include assessing the effects of defects on the thermal expansion and how this in turn may affect the interpretation of chemical expansion and defect thermodynamics. We have chosen to study the state of the art proton conducting perovskite $BaCeO_3$, which has already been studied extensively in terms of hydration,[8–14] thus serving as a good comparative basis for the present work.

2. Methodology

Thermodynamic formalism

Vibrational thermodynamics and thermal properties of solids can be calculated by evaluating their phonon density of states. In the harmonic approximation and under constant volume, the phonon contributions to the Helmholtz energy, F^{vib}, are given by;

$$F^{vib} = \sum_{\boldsymbol{q},\nu} \frac{\hbar\omega(\boldsymbol{q},\nu)}{2} + k_B T \sum_{\boldsymbol{q},\nu} \ln(1 - \exp(-\hbar\omega(\boldsymbol{q},\nu)/k_B T)) \quad (4)$$

where $\boldsymbol{q}$ and ν are the wave vector and band index, respectively while $\omega(\boldsymbol{q},\nu)$ is the phonon frequency at the specific $\boldsymbol{q}$ and ν.

As an approach to include anharmonic effects, we here adopt the quasiharmonic approximation,[15,16] hereafter referred to as QHA. The Gibbs free energy, $G(T,p)$, is taken as the unique minimum of the sum of the total electronic energy, $E^{el}(V)$, the Helmholtz vibrational energy, F^{vib}, and pV work with respect to volume given by:

$$G(T,p) = \min_V \left[E^{el}(V) + F^{vib}(T;V) + pV \right] \quad (5)$$

It should be noted that for each p and V, the function inside the square brackets of (5) is minimised with respect to volume. F^{vib} is assumed to only be a function of temperature at each specific volume. By fitting the thermodynamic functions on the right hand side of (5) to the third order Birch–Murnaghan isothermal equation of state (B–M EoS),[17] Gibbs free energies at finite temperatures are obtained allowing the evaluation of all thermal properties as a function of temperature and pressure. The fitting procedure is demonstrated in Fig. 1 for bulk $BaCeO_3$ where a fully isotropic expansion has been chosen. The calculated values of $E^{el}(V) + F^{vib}(T;V)$ are plotted as a function of the unit cell volume at 100 K intervals between 0 and 1000 K. The solid lines represent the fits from the B–M EoS. Corresponding equilibrium volumes and isothermal bulk moduli are obtained simultaneously from this fitting procedure. The entropy (S) and
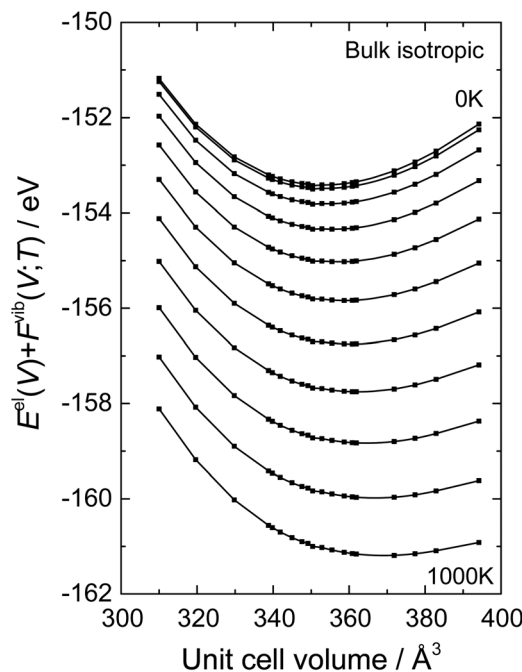

Fig. 1 $E^{el}(V) + F^{vib}(T;V)$ as a function of the unit cell volume for 0–1000 K with temperature intervals of 100 K of bulk $BaCeO_3$ where a fully isotropic expansion has been chosen. The points denote calculated values of $E^{el}(V) + F^{vib}(T;V)$ while the solid lines are fitted by the Birch–Murnaghan third order equation of state.

heat capacity at constant pressure (C_p) are then given by the first and second order partial derivatives of $G(T,p)$ with respect to T, respectively.

The free energy of defect formation ($\Delta_F F_{defect}$ or $\Delta_F G_{defect}$) is given by;

$$\Delta_F G_{defect} = \Delta E_{defect}^{tot} + \Delta_F G_{defect}^{vib}$$
$$- \sum_i \Delta n_i \mu_i(T,p) + q_i(\varepsilon_f + \Delta\varepsilon) + p\Delta_F V_{defect} \quad (6)$$

where ΔE_{defect}^{tot} denotes the total electronic energy difference between the defective and pristine supercell, while $\Delta_F G_{defect}^{vib}$ (or $\Delta_F F_{defect}^{vib}$) is the vibrational (phonon) contribution to the free energy of formation. Δn_i is the change in the number of defects i with chemical potential, μ_i, while q_i is the effective charge of the defect and ε_f is the Fermi level. $\Delta\varepsilon$ is the shift in the core potentials of the perfect and defective supercell to correct for shifts in the band edges due to the jellium background charge while $p\Delta_F V_{defect}$ represents the contributions from the pressure and defect formation volume under zero/constant pressure conditions. Further, the chemical potential of gaseous species, i, is defined by:

$$\mu_i(T,p_i) = \mu_i^\circ + H_i^{zpe} + H_i^\circ(T) - TS_i^\circ(T) + k_B T \ln\left(\frac{p_i}{p^\circ}\right) \quad (7)$$

where μ_i° is set to the total electronic energy of the isolated i-molecule as determined by DFT. H_i^{zpe} is the zero-point energy obtained from experimental vibrational frequencies, while $H_i^\circ(T)$ and $S_i^\circ(T)$ are taken from the HSC 8.2.0 database.[18] p_i is the partial pressure of i while p° is the standard pressure (1 bar).

This journal is © the Owner Societies 2016

Phys. Chem. Chem. Phys., 2016, **18**, 31296–31303 | **31297**

Computational methodology

All first principles calculations in this work have been performed within the Density Functional Theory (DFT) formalism as implemented in the VASP code.[19] Both the LDA[20] and GGA-PBE[21] functionals have been used and the core potentials were treated using the projector-augmented wave (PAW) method.[22] The electronic wave functions were expanded using a set of plane waves with a constant cut-off energy of 500 eV. The defect calculations were performed using both $2 \times 1 \times 2$ (80 atoms) and $2 \times 2 \times 2$ (160 atoms) supercell expansions of the experimentally determined orthorhombic *Pnma* BaCeO$_3$ 20 atom unit cell.[23] Electronic integrations over the Brillouin zone were performed using a $4 \times 4 \times 4$ Monkhorst–Pack k-mesh for the unit cell,[24] and reduced accordingly for larger supercells. To ensure sufficient convergence of the calculated forces, all calculations were performed with ionic and electronic convergence criteria of 10^{-4} eV Å^{-1} and 10^{-8} eV, respectively.

Orthorhombic BaCeO$_3$ exhibits two structurally inequivalent oxygen sites; an apical oxygen site occupying Wyckoff position 4c and an equatorial site occupying the Wyckoff position 8d. Previous work[8,14] has demonstrated that both protons and oxygen vacancies are most stable at the 4c site, and we have therefore only considered this site for both defects. For all charged defects, the total charge of the supercells was adjusted to simulate the desired charge state, by the standard means of charge-compensation with a homogenous jellium charge. Note that we have explicitly not included any acceptors in the supercells due to the large computational demand that would impose. While this is perfectly reasonable in a dilute limit with few defects, thermodynamics and thermal properties may be influenced by the type and amount of acceptor at higher doping levels ($\geq$10 mol%).[8,25–27] Further work is needed to assess such dopant effects.

The phonon frequencies were obtained from the Hellmann–Feynman forces acting on all ions within the harmonic (HA) and quasiharmonic approximations (QHA) using finite displacements of ± 0.01 Å as implemented in the Phonopy code.[15,16,28] For the QHA calculations, lattice parameters were varied isotropically up to $\pm 4\%$ using up to 20 volume points. For the defective cells, the phonon spectra are only evaluated at the Γ-point due to the large size of the supercells.

3. Results and discussion

Thermal and chemical expansion of orthorhombic BaCeO$_3$

The heat capacities at constant pressure, C_p, and constant volume, C_V, for isotropic defect-free bulk BaCeO$_3$ as a function of temperature are displayed in Fig. 2 along with experimental values for C_p.[29–31] The heat capacities for bulk BaCeO$_3$ are in good agreement with the experimental values from literature obeying the classical Debye law at the lowest temperatures where the heat capacities exhibit a T^3-dependency.[32] At higher temperatures (above 400 K), C_V approaches a constant value of $3N \times R$ ($\sim$125 J K^{-1} mol^{-1}) as per the Dulong–Petit law, where N is the number of atoms per formula unit (5 for BaCeO$_3$). The calculated C_p maintains a positive slope and starts deviating from the
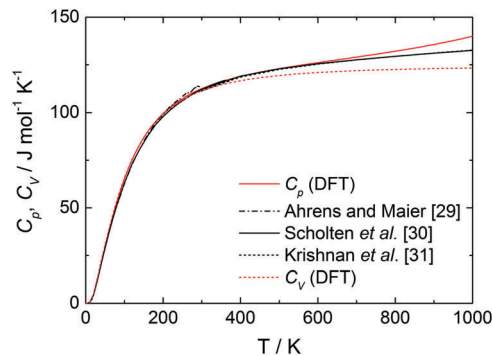

Fig. 2 Heat capacity at constant pressure, C_p (red solid), and volume, C_V (red dotted), as a function of temperature along with experimental values for C_p.[29–31] (black).

literature values at $T \sim 600$ K with values being higher than those reported from experiments. The difference between the calculated and experimentally determined C_p-values could stem from the fact that BaCeO$_3$ undergoes several phase changes in the temperature range measured,[9,33,34] and may as such display different C_p values than the orthorhombic *Pnma* phase used for the DFT calculations. This is also in accordance with work by Ligny and Richet[35] on SrZrO$_3$ in which the high temperature cubic polymorph ($Pm\bar{3}m$) was shown to exhibit an apparent lower heat capacity than its low temperature orthorhombic ground state structure.

The linear thermal expansion of BaCeO$_3$ and the resulting linear thermal expansion coefficients, α_i, given by (3), are shown in Fig. 3(a) and (b), respectively. Note that all linear thermal expansion coefficients are given by $\frac{1}{l}\frac{\partial l}{\partial T}$ where $l = V^{\frac{1}{3}}$, *i.e.* we only evaluate a single average coefficient for each expansion. We also assess the effect of an oxygen vacancy and a proton on the thermal expansion. As the figure demonstrates, the linear thermal expansion coefficient, α_i, for the pristine and defective BaCeO$_3$ cells becomes increasingly positive with temperature. All coefficients at lower temperatures (300–600 K) are in reasonable agreement with literature values on undoped and acceptor doped BaCeO$_3$ determined by dilatometry and XRD; 8–14 $\times 10^{-6}$ K^{-1}.[1,2,36–40] At higher temperatures (600–1000 K), the calculated thermal expansion coefficients vary from 13 to 27 $\times 10^{-6}$ K^{-1}, and are somewhat higher than corresponding values from literature. This difference is likely to stem from phase transitions to other high temperature polymorphs as for instance dilatometry measurements on BaCe$_{0.8-x}$Zr$_x$Y$_{0.2}$O$_{3-\delta}$ ($x \leq 0.4$) have been shown to yield different α_i-values above and below $\sim$600 °C.[39,40] Computational studies on other oxides such as CeO$_2$ and SrTiO$_3$ have also shown that the GGA functional tends to overestimate the thermal expansion coefficient.[35,41,42]

Interestingly, the supercells containing defects both display lower α-values compared to bulk BaCeO$_3$, which arguably stems from a blue shift of the phonon spectra due to their negative formation volumes (-20.4 and -6.8 Å^3 for $v_O^{\bullet\bullet}$ and OH$_O^\bullet$, respectively). There is also a significant difference in the thermal expansion coefficients between the cells containing $v_O^{\bullet\bullet}$ and OH$_O^\bullet$ demonstrating that BaCeO$_3$ may thermally expand

31298 | *Phys. Chem. Chem. Phys.*, 2016, **18**, 31296–31303
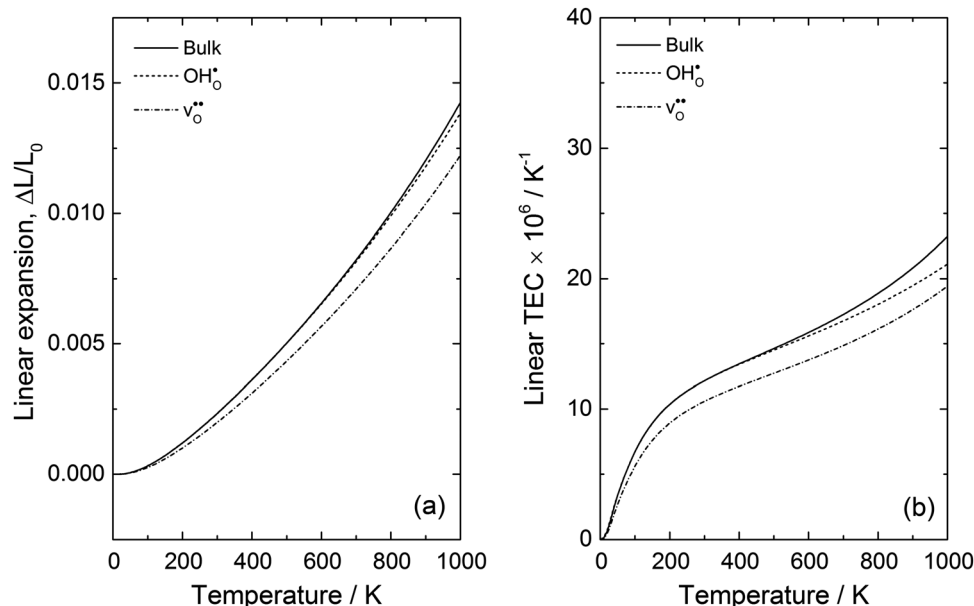
This journal is © the Owner Societies 2016

Fig. 3 (a) Linear thermal expansion of bulk $BaCeO_3$ with or without any defects and (b) the resulting thermal expansion coefficients determined by quasiharmonic first principles phonon calculations. For the defective systems, a single oxygen vacancy, $v_O^{\bullet\bullet}$, or proton, $OH_O^{\bullet}$ has been investigated. All lattice parameters have been varied isotropically and linear thermal expansion coefficients are given by $\frac{1}{l}\frac{\partial l}{\partial T}$ where $l = V^{\frac{1}{3}}$.

differently depending on the water vapour partial pressure employed. This is also in good correspondence with recent work on similar compositions.[1,2,43] Drawing any overall conclusions regarding the effect of ionic defects on thermal expansion is difficult based on the present work alone, but there appears to be a correlation between the defect formation volume (or defect chemical expansion coefficient) and the change in the thermal expansion coefficient. For instance, the cell containing a proton or an oxygen vacancy, which both display negative formation volumes, also exhibit lower thermal expansion coefficients than that of the pristine system. This could suggest that defects with positive formation volumes, such as large acceptor dopants[44] or neutral oxygen vacancies,[45] may increase the thermal expansion coefficient. This opens up for the possibility of altering the thermal expansion of a material system simply by changing its defect structure, and may help in limiting thermal mismatch in device fabrication.

The chemical expansion coefficient due to hydration per mole oxygen vacancy, ε_{hydr}, is given by the relative difference of the chemical expansion coefficients for the formation of an oxygen vacancy and a proton, $\varepsilon_{v_O^{\bullet\bullet}}$ and $\varepsilon_{OH_O^{\bullet}}$, respectively:

$$\varepsilon_{hydr} = 2\varepsilon_{OH_O^{\bullet}} - \varepsilon_{v_O^{\bullet\bullet}} \tag{8}$$

Thus, ε_{hydr} is calculated with respect to the defect-free lattice, while experimental determination of ε_{hydr} uses the volume differences between the hydrated and dry lattice *i.e.* relative to the defective lattice. To assess the effect of such differences, we calculate ε_{hydr} in three separate ways;

$$\varepsilon_{hydr,1} = \frac{2}{[OH_O^{\bullet}]}\left(\frac{2V_{OH_O^{\bullet}} - V_{v_O^{\bullet\bullet}} - V_{bulk}}{V_{bulk}}\right) \tag{9}$$

$$\varepsilon_{hydr,2} = \frac{2}{[OH_O^{\bullet}]}\left(\frac{\left(V_{OH_O^{\bullet}} - V_{bulk}\right) + \left(V_{OH_O^{\bullet}} - V_{v_O^{\bullet\bullet}}\right)}{V_{v_O^{\bullet\bullet}}}\right) \tag{10}$$

$$\varepsilon_{hydr,3} = \frac{2}{[OH_O^{\bullet}]}\left(\frac{V_{2OH_O^{\bullet}} - V_{v_O^{\bullet\bullet}}}{V_{v_O^{\bullet\bullet}}}\right) \tag{11}$$

where $V_{OH_O^{\bullet}}$, $V_{v_O^{\bullet\bullet}}$ and $V_{2OH_O^{\bullet}}$ denote the equilibrium supercell volumes with a proton, oxygen vacancy, and 2 protons in the same supercell, respectively, while V_{bulk} represents the volume of the pristine lattice. In all three cases, ε_{hydr} was determined to be virtually identical yielding a maximum difference of a mere 2% suggesting that all calculated chemical expansion coefficients, regardless of calculation method, should be comparable to experiments. Fig. 4 displays $\varepsilon_{v_O^{\bullet\bullet}}$ and $\varepsilon_{OH_O^{\bullet}}$, and the resulting chemical expansion coefficient upon hydration calculated by (9), ε_{hydr}, as a function of temperature. Note that we have chosen to plot the individual contributions to ε_{hydr}, *i.e.* $2\varepsilon_{OH_O^{\bullet}}$ and $-\varepsilon_{v_O^{\bullet\bullet}}$. As the figure demonstrates, the chemical expansion coefficient for the supercells containing $v_O^{\bullet\bullet}$ and $OH_O^{\bullet}$ becomes increasingly negative with increasing temperature. The resulting chemical expansion coefficient due to hydration varies to a much smaller extent, ranging from 0.070 to 0.115 in the temperature range presented. This is in reasonable agreement with other experimental and computational work.[1,12,38]

Given that ε_{hydr} varies with temperature, distinctly different volume expansions are expected when hydrating acceptor doped $BaCeO_3$ isothermally at different temperatures; 0.35 to 0.58% for 10 mol%. The results presented here can thus partially explain the large scatter in chemical expansion coefficients due to hydration found experimentally. For instance, the difference
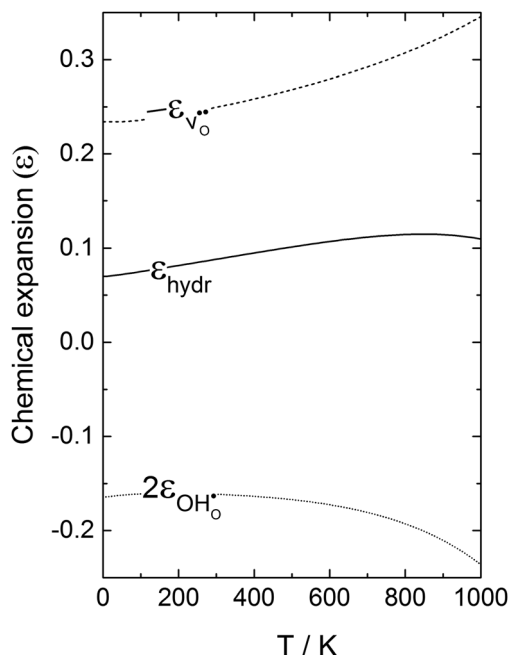
Fig. 4 Chemical expansion coefficient due to hydration, $\varepsilon_{\text{hydr}}$, and its individual contributions $-\varepsilon_{\text{v}_{\text{O}}^{\bullet\bullet}}$ and $2\varepsilon_{\text{OH}_{\text{O}}^{\bullet}}$, as calculated by quasiharmonic phonon calculations as a function of temperature.

in $\varepsilon_{\text{hydr}}$ of 20 mol% acceptor doped BaCeO$_3$ determined by Yamaguchi and Yamada[38] and Andersson *et al.*[1] (0.096 and 0.151, respectively) could stem from the differences in the water vapour partial pressures ($p_{\text{H}_2\text{O}}$) used during heating and cooling. While Yamaguchi and Yamada[38] humidified the gas with a constant $p_{\text{H}_2\text{O}}$ of $\sim$0.03 atm, Andersson *et al.*[1] were not able to monitor or control $p_{\text{H}_2\text{O}}$ but estimated it to be around 10^{-4} atm based on the volume expansion/contraction onset and the material's hydration thermodynamics. Such a large difference in $p_{\text{H}_2\text{O}}$ means that the material will hydrate (or dehydrate) in different temperature intervals, and the corresponding difference in lattice expansion will thus be affected due to the temperature dependency of $\varepsilon_{\text{hydr}}$. Consequently, careful attention to the experimental conditions is needed when comparing specific chemical expansion coefficients extracted.

By combining the expressions for the thermal and chemical expansion coefficient, (3) and (1), respectively, a full description of the thermochemical lattice expansion of BaCeO$_3$ as a function of temperature can be obtained. This requires an expression for the proton concentration as a function of temperature. For that purpose, we will firstly assume that the effectively negative charged acceptors, Acc$'$, are fully charge compensated by oxygen vacancies and/or protons *i.e.* all other defects are considered to have negligible concentrations:

$$[\text{Acc}'] = [\text{OH}_{\text{O}}^{\bullet}] + 2[\text{v}_{\text{O}}^{\bullet\bullet}] \quad (12)$$

Secondly, the oxygen site restriction for perovskites is imposed:

$$3 = [\text{O}_{\text{O}}^{\times}] + [\text{OH}_{\text{O}}^{\bullet}] + [\text{v}_{\text{O}}^{\bullet\bullet}] \quad (13)$$

The proton concentration is then determined by a combination of (12) and (13) along with the hydration equilibrium constant,

K_{hydr}, for reaction (2), for undoped BaCeO$_3$. For any further information regarding the hydration thermodynamics, the reader is referred to work by Bjørheim *et al.*[12] The volumetric thermal expansion coefficient upon hydration, α, is assumed to change linearly from the thermal expansion coefficient of the oxygen vacancy, $\alpha_{\text{v}_{\text{O}}^{\bullet\bullet}}$, to that of the proton, $\alpha_{\text{OH}_{\text{O}}^{\bullet}}$:

$$\alpha = \alpha_{\text{v}_{\text{O}}^{\bullet\bullet}} \frac{([\text{Acc}'] - [\text{OH}_{\text{O}}^{\bullet}])}{[\text{Acc}']} + \frac{[\text{OH}_{\text{O}}^{\bullet}]}{[\text{Acc}']} \alpha_{\text{OH}_{\text{O}}^{\bullet}} \quad (14)$$

The linear relationship in (14) is from the simple rule of mixtures, often used in predicting thermal and mechanical properties of composite materials. It assumes that the physical properties of each phase are not influenced by each other's presence in the mixture.[46,47] By combining the expressions for the thermal and chemical expansion coefficient upon hydration (*cf.* Fig. 4), the thermochemical expansion of the BaCeO$_3$ unit cell can now be determined where the unit cell volume at temperature T_{f}, V_{f}, is given by:

$$V_{\text{f}} = V_i + \alpha(T_{\text{f}} - T_i)V_i + \frac{1}{2}\varepsilon_{\text{hydr}}^0 \left([\text{OH}_{\text{O}}^{\bullet}]_{\text{f}} - [\text{OH}_{\text{O}}^{\bullet}]_i\right)V_i \quad (15)$$

V_i represents the unit cell volume of the dehydrated system at T_i, while $[\text{OH}_{\text{O}}^{\bullet}]_{\text{f}}$ and $[\text{OH}_{\text{O}}^{\bullet}]_i$ denote the proton concentration at T_{f} and T_i, respectively. Note that we have chosen to use a constant value for the chemical expansion coefficient, $\varepsilon_{\text{hydr}}^0$, which differs from $\varepsilon_{\text{hydr}}$, given in (8), in that it is entirely temperature independent stemming from the equilibrium volumes of all supercells calculated at 0 K and excludes all zero-point energy contributions (0.078). This is intentionally done to avoid double counting the temperature dependencies of the equilibrium volumes, which is already implemented in the thermal expansion coefficient in (14). Fig. 5a displays the change in the unit cell volume as a function of temperature for different acceptor dopant concentrations (5–20 mol%) under humid conditions, $p_{\text{H}_2\text{O}}$ = 0.025 atm, while Fig. 5b gives the unit cell volume for 20 mol% doped BaCeO$_3$ where $p_{\text{H}_2\text{O}}$ is varied from 0.025 to 1 atm. Fig. 5a demonstrates that the volume increases to a larger extent upon hydration with increasing doping concentrations reflecting higher proton concentrations. While the unit cell volume only changes gradually upon hydration (or dehydration) for the lower doping concentrations (5–15 mol%), the volume change for 20 mol% doped BaCeO$_3$ is more abrupt, and the volume is almost constant in a small temperature interval for 20 mol% doped BaCeO$_3$. In Fig. 5b, protons are retained to higher temperatures for $p_{\text{H}_2\text{O}}$ = 1 atm and further heating is therefore needed for the volume to decrease compared to the corresponding unit cell volume at $p_{\text{H}_2\text{O}}$ = 0.025 atm. Fig. 5b shows an additional interesting feature where the volume of the unit cell is not the same at lower temperatures ($<$600 K) when the water vapour partial pressure is changed. This stems from the difference in the thermal expansion coefficients upon hydration (*cf.* Fig. 3) where the unit cell at $p_{\text{H}_2\text{O}}$ = 1 atm is thermally contracting to a larger extent than the corresponding unit cell at 0.025 atm.

As both the chemical and thermal expansion coefficients change as a function of temperature, and the two processes
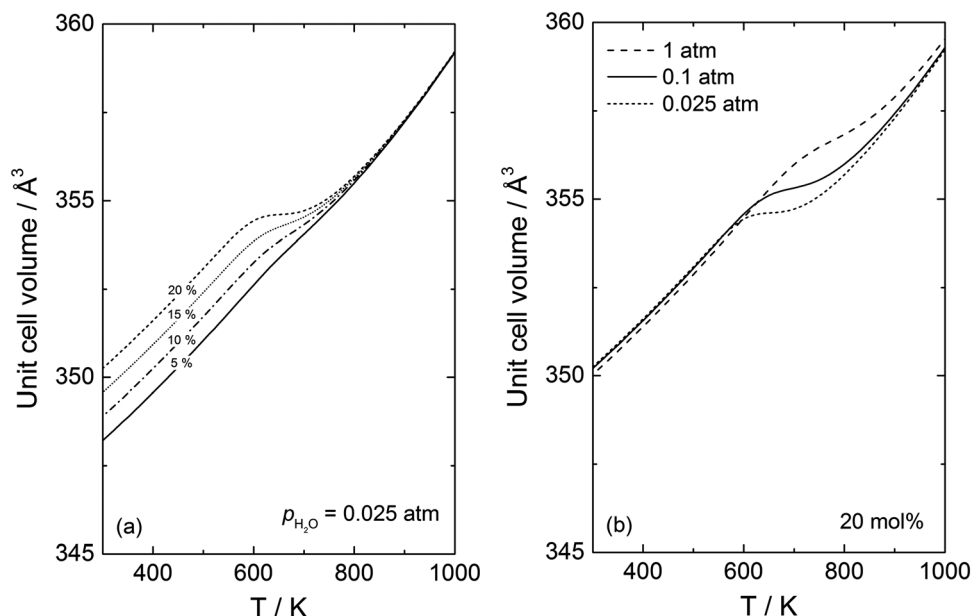
31300 | *Phys. Chem. Chem. Phys.*, 2016, **18**, 31296–31303

This journal is © the Owner Societies 2016

Fig. 5 Unit cell volume of BaCeO$_3$ calculated using the quasiharmonic approximation as a function of temperature for (a) different acceptor concentrations (5–20 mol%) for p_{H_2O} = 0.025 atm and (b) 20 mol% acceptor doped BaCeO$_3$ under different water vapour partial pressures (0.025–1 atm).

are interrelated, their accurate determination through experiments may be difficult. Through the present DFT calculations, we are able to decouple the expansion mechanisms, demonstrating that experimental work may easily over- or underestimate the chemical expansion coefficient. Since α for a protonated cell is higher than the corresponding cell with an oxygen vacancy (Fig. 3), the lattice will in fact thermally contract to a larger extent upon cooling for a hydrated material. This, in turn, means that the chemical expansion coefficient determined experimentally will be grossly underestimated, as it is often assumed that the difference in the volume under wet and dry conditions at lower temperatures is only given by chemical expansion. For 20 mol% acceptor doped BaCeO$_3$, this results in an apparent chemical expansion coefficient of 0.056 at 300 K whereas the actual coefficient is far higher (0.078) i.e. an underestimation of 27%. This discrepancy increases with decreasing acceptor concentrations yielding an underestimation of 55% at 300 K for 10 mol%. This underestimation can for instance help explain the large

scatter in the chemical expansion coefficients determined experimentally, which for acceptor doped BaCeO$_3$, vary between 0.030 and 0.151.[1,38]

Defect thermodynamics of bulk BaCeO$_3$

The thermochemical expansion of BaCeO$_3$ will undoubtedly affect the defect thermodynamics due to changes it will impose on the phonon spectra. While most of the defect thermodynamics have already been treated in our previous contribution using the harmonic approximation (HA),[12] this work assumed that the defects themselves did not affect thermal expansion. We are, thus, only determining the effect of anharmonicity on the thermodynamics by using the QHA, and the reader is referred to ref. 12 for further details on the thermodynamic formalism and defect thermodynamics of BaCeO$_3$ and other perovskite oxides. As the results herein were obtained using 2 × 1 × 2 supercells (80 atoms), we first assess the effect of the supercell size on the thermodynamics. Fig. 6 shows (a) the calculated vibrational formation
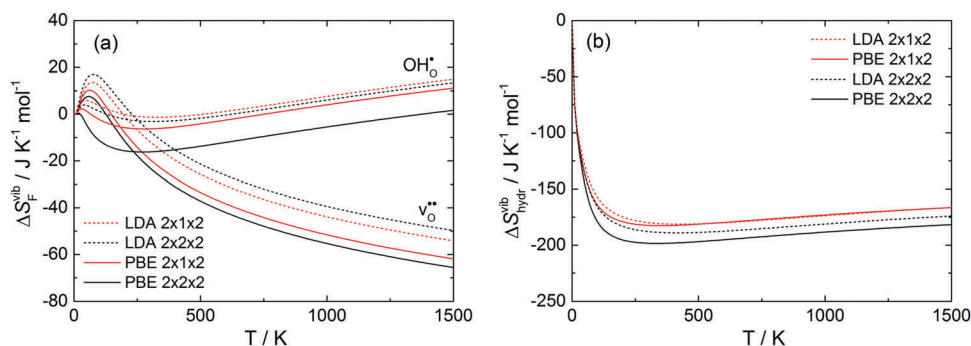

Fig. 6 (a) Vibrational formation entropy for an oxygen vacancy and proton and (b) the resulting hydration entropy determined by harmonic phonon calculations for BaCeO$_3$ with different supercell sizes and functionals.
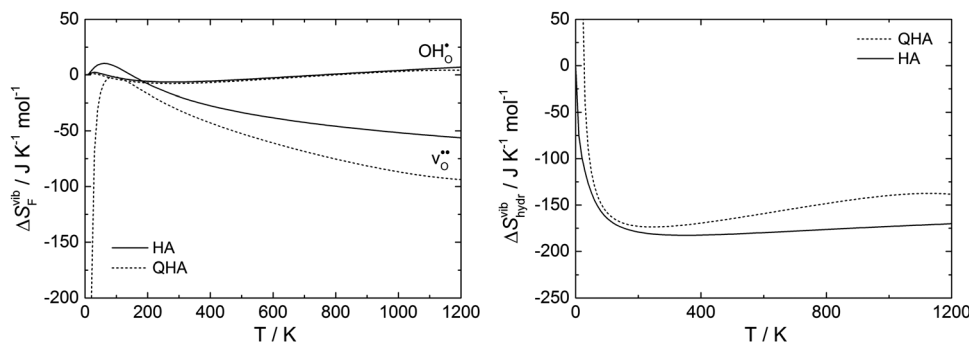
This journal is © the Owner Societies 2016

Phys. Chem. Chem. Phys., 2016, **18**, 31296–31303 | **31301**

Fig. 7 Vibrational formation entropy for an oxygen vacancy and a proton, and the entropy of hydration for BaCeO$_3$, as a function of temperature calculated by the harmonic and quasiharmonic approximations, HA and QHA, respectively. The latter also accounts for the volume dependency of the phonon spectra.

entropies of an oxygen vacancy and proton while (b) shows the resulting hydration entropies using the LDA and PBE functional and 2 × 1 × 2 and 2 × 2 × 2 supercells from phonon calculations within the harmonic approximation as a function of temperature. Both functionals and supercells yield similar values with the entropies generally being slightly more negative for larger supercells and with the PBE functional.

Fig. 7 displays the vibrational formation entropy for an oxygen vacancy and proton, along with the resulting hydration entropy for BaCeO$_3$, as a function of temperature calculated by the HA and the QHA where the latter accounts for the volume dependency of the phonons. While there is virtually no difference in the proton formation entropy calculated by the two approximations, the oxygen vacancy formation entropy differs by almost 35 J K^{-1} mol^{-1} at 1000 K. This difference could among other things stem from assuming, in the HA, that the partial derivative of the entropy with respect to volume, $\left(\frac{\partial S}{\partial V}\right)$, does not change upon defect formation;[12,41,48–51]

$$\left(\frac{\partial S}{\partial V}\right)_{\text{def}} = \left(\frac{\partial S}{\partial V}\right)_{\text{bulk}} \quad (16)$$

Under constant pressure, $\left(\frac{\partial S}{\partial V}\right)$ is further given by

$$\left(\frac{\partial S}{\partial V}\right)_p = \alpha_V \beta_T \quad (17)$$

where α_V and β_T are the volumetric thermal expansion coefficient and isothermal bulk modulus, respectively. Thus, for this assumption to be valid, the product $\alpha_V \beta_T$ should not change upon defect formation. However, through the present work using the QHA, the thermal expansion coefficient has been shown to change significantly when defects are introduced, especially in the case of oxygen vacancies, relative to the pristine system (Fig. 3). This could thus explain the difference in the oxygen vacancy formation entropies calculated using the two approximations. Whether one could alleviate the differences between the approximations by using larger supercells in the calculations, i.e. more dilute defect concentrations, remains unkown but more work is needed to address these aspects further. Interestingly, for the

hydration entropy, which is calculated by subtracting the defect formation entropies through $\Delta S_{\text{hydr}}^{\text{vib}} = \Delta S_{\text{v}_O^{\bullet\bullet}}^{\text{vib}} - \Delta S_{\text{OH}_O^{\bullet}}^{\text{vib}} - S_{\text{H}_2\text{O}}^{\circ}$, the difference between the approximations again only stems from the oxygen vacancy formation entropy reaching a maximum difference of about 35 J K^{-1} mol^{-1} at higher temperatures. Ultimately, we find that most of the vibrational thermodynamics are appropriately described by the HA as anharmonic effects appear to be of a minor concern.

4. Conclusions

In the present contribution we have investigated the thermal and chemical expansion of BaCeO$_3$ from first principles phonon calculations. This has allowed us, for the first time, to decouple these expansion processes providing fundamental insights to lattice expansion. The calculations reveal that the formation of defects such as oxygen vacancies or protons can play a significant role in thermal expansion displaying lower thermal expansion coefficients compared to that of the defect-free bulk. Further, due to the differences in the thermal expansion coefficients between the dry and protonated unit cell, we demonstrate that experimentally determined chemical expansion coefficients due to hydration can be grossly underestimated being around 55% lower in the case of 10 mol% acceptor doped BaCeO$_3$. The chemical expansion coefficient is also found to change with temperature ranging between 0.070 and 0.115 per mole oxygen vacancy thus demonstrating that different experimental conditions can significantly change the chemical expansion of the lattice. Overall, our results rationalise the large scatter in the chemical expansion coefficients determined experimentally, which for acceptor doped BaCeO$_3$ varies from 0.030 to 0.151 per mole oxygen vacancy. Lastly, we have assessed how thermochemical expansion may influence the defect thermodynamics by including the volume dependency of the phonon spectra.

Acknowledgements

References

1 A. K. E. Andersson, S. M. Selbach, C. S. Knee and T. Grande, *J. Am. Ceram. Soc.*, 2014, **97**, 2654–2661.

2 G. C. Mather, G. Heras-Juaristi, C. Ritter, R. O. Fuentes, A. L. Chinelatto, D. Pérez-Coll and U. Amador, *Chem. Mater.*, 2016, **28**, 4292–4299.

3 D. Marrocchelli, S. R. Bishop and J. Kilner, *J. Mater. Chem. A*, 2013, **1**, 7673–7680.

4 D. Marrocchelli, N. H. Perry and S. R. Bishop, *Phys. Chem. Chem. Phys.*, 2015, **17**, 10028–10039.

5 D. Marrocchelli, S. R. Bishop, H. L. Tuller and B. Yildiz, *Adv. Funct. Mater.*, 2012, **22**, 1958–1965.

6 S. R. Bishop, D. Marrocchelli, C. Chatzichristodoulou, N. H. Perry, M. B. Mogensen, H. L. Tuller and E. D. Wachsman, *Annu. Rev. Mater. Res.*, 2014, **44**, 205–239.

7 S. R. Bishop, D. Marrocchelli, W. Fang, K. Amezawa, K. Yashiro and G. W. Watson, *Energy Environ. Sci.*, 2013, **6**, 1142–1146.

8 A. Løken, T. S. Bjørheim and R. Haugsrud, *J. Mater. Chem. A*, 2015, **3**, 23289–23298.

9 K. S. Knight, *Solid State Ionics*, 1994, **74**, 109–117.

10 M. Oishi, K. Yashiro, K. Sato, J. Mizusaki, N. Kitamura, K. Amezawa, T. Kawada and Y. Uchimoto, *Solid State Ionics*, 2008, **179**, 529–535.

11 K. D. Kreuer, *Solid State Ionics*, 1999, **125**, 285–302.

12 T. S. Bjørheim, A. Løken and R. Haugsrud, *J. Mater. Chem. A*, 2016, **4**, 5917–5924.

13 M. Oishi, S. Akoshima, K. Yashiro, K. Sato, J. Mizusaki and T. Kawada, *Solid State Ionics*, 2009, **180**, 127–131.

14 J. Hermet, F. Bottin, G. Dezanneau and G. Geneste, *Phys. Rev. B: Condens. Matter Mater. Phys.*, 2012, **85**, 205137.

15 A. Togo and I. Tanaka, *Scr. Mater.*, 2015, **108**, 1–5.

16 A. Togo, L. Chaput, I. Tanaka and G. Hug, *Phys. Rev. B: Condens. Matter Mater. Phys.*, 2010, **81**, 174301.

17 F. Birch, *Phys. Rev.*, 1947, **71**, 809–824.

18 HSC Chemistry 8.2.0, Outetec Technologies, 2015.

19 G. Kresse and J. Furthmüller, *Phys. Rev. B: Condens. Matter Mater. Phys.*, 1996, **54**, 11169–11186.

20 W. Kohn and L. J. Sham, *Phys. Rev.*, 1965, **140**, A1133–A1138.

21 J. P. Perdew, K. Burke and M. Ernzerhof, *Phys. Rev. Lett.*, 1996, **77**, 3865–3868.

22 G. Kresse and D. Joubert, *Phys. Rev. B: Condens. Matter Mater. Phys.*, 1999, **59**, 1758–1775.

23 K. S. Knight and N. Bonanos, *J. Mater. Chem.*, 1994, **4**, 899–901.

24 H. J. Monkhorst and J. D. Pack, *Phys. Rev. B: Condens. Matter Mater. Phys.*, 1976, **13**, 5188–5192.

25 A. Løken, S. W. Saeed, M. N. Getz, X. Liu and T. S. Bjørheim, *J. Mater. Chem. A*, 2016, **4**, 9229–9235.

26 A. Løken, C. Kjølseth and R. Haugsrud, *Solid State Ionics*, 2014, **267**, 61–67.

27 K. D. Kreuer, S. Adams, W. Münch, A. Fuchs, U. Klock and J. Maier, *Solid State Ionics*, 2001, **145**, 295–306.

28 A. Togo, F. Oba and I. Tanaka, *Phys. Rev. B: Condens. Matter Mater. Phys.*, 2008, **78**, 134106.

29 M. Ahrens and J. Maier, *Thermochim. Acta*, 2006, **443**, 189–196.

30 M. J. Scholten, J. Schoonman, J. C. v. Miltenburg and E. H. P. Cordfunke, *Thermochim. Acta*, 1995, **268**, 161–168.

31 R. Venkata Krishnan, K. Nagarajan and P. R. Vasudeva Rao, *J. Nucl. Mater.*, 2001, **299**, 28–31.

32 P. Debye, *Ann. Phys.*, 1912, **344**, 789–839.

33 V. M. Egorov, Y. M. Baikov, N. F. Kartenko, B. T. Melekh and Y. N. Filin, *Phys. Solid State*, 1998, **40**, 1911–1914.

34 T. Ohzeki, S. Hasegawa, M. Shimizu and T. Hashimoto, *Solid State Ionics*, 2009, **180**, 1034–1039.

35 D. de Ligny and P. Richet, *Phys. Rev. B: Condens. Matter Mater. Phys.*, 1996, **53**, 3013–3022.

36 J.-X. Wang, L.-P. Li, B. J. Campbell, Z. Lv, Y. Ji, Y.-F. Xue and W.-H. Su, *Mater. Chem. Phys.*, 2004, **86**, 150–155.

37 S. Yamanaka, M. Fujikane, T. Hamaguchi, H. Muta, T. Oyama, T. Matsuda, S.-i. Kobayashi and K. Kurosaki, *J. Alloys Compd.*, 2003, **359**, 109–113.

38 S. Yamaguchi and N. Yamada, *Solid State Ionics*, 2003, **162–163**, 23–29.

39 Y. G. Lyagaeva, D. A. Medvedev, A. K. Demin, P. Tsiakaras and O. G. Reznitskikh, *Phys. Solid State*, 2015, **57**, 285–289.

40 J. Lagaeva, D. Medvedev, A. Demin and P. Tsiakaras, *J. Power Sources*, 2015, **278**, 436–444.

41 S. Grieshammer, T. Zacherle and M. Martin, *Phys. Chem. Chem. Phys.*, 2013, **15**, 15935–15942.

42 Y. Lu, D. Jia, F. Gao, T. Hu and Z. Chen, *Solid State Commun.*, 2015, **201**, 25–30.

43 C. Hiraiwa, D. Han, A. Kuramitsu, A. Kuwabara, H. Takeuchi, M. Majima and T. Uda, *J. Am. Ceram. Soc.*, 2013, **96**, 879–884.

44 E. Jedvik, A. Lindman, M. Þ. Benediktsson and G. Wahnström, *Solid State Ionics*, 2015, **275**, 2–8.

45 T. S. Bjørheim, M. Arrigoni, D. Gryaznov, E. Kotomin and J. Maier, *Phys. Chem. Chem. Phys.*, 2015, **17**, 20765–20774.

46 H. A. Bruck and B. H. Rabin, *J. Am. Ceram. Soc.*, 1999, **82**, 2927–2930.

47 H. S. Kim, S. I. Hong and S. J. Kim, *J. Mater. Process. Technol.*, 2001, **112**, 109–113.

48 T. S. Bjørheim, E. A. Kotomin and J. Maier, *J. Mater. Chem. A*, 2015, **3**, 7639–7648.

49 P. Ágoston and K. Albe, *Phys. Chem. Chem. Phys.*, 2009, **11**, 3226–3232.

50 Y. Mishin, M. R. Sørensen and A. F. Voter, *Philos. Mag. A*, 2001, **81**, 2591–2612.

51 T. Zacherle, P. C. Schmidt and M. Martin, *Phys. Rev. B: Condens. Matter Mater. Phys.*, 2013, **87**, 235206.

This journal is © the Owner Societies 2016

Phys. Chem. Chem. Phys., 2016, **18**, 31296–31303 | **31303**